Applied Physics Letters

Assessing the electro-deformation and electro-poration of biological cells using a three-dimensional finite element model

Cite as: Appl. Phys. Lett. **114**, 063701 (2019); https://doi.org/10.1063/1.5079292
Submitted: 30 October 2018 . Accepted: 18 January 2019 . Published Online: 11 February 2019

D. Shamoon, J. Dermol-Černe, L. Rems, M. Reberšek, T. Kotnik, S. Lasquellec, C. Brosseau, and D. Miklavčič

AIP Publishing

Applied Physics Letters ARTICLE scitation.org/journal/apl

Assessing the electro-deformation and electro-poration of biological cells using a three-dimensional finite element model

Cite as: Appl. Phys. Lett. **114**, 063701 (2019); doi: 10.1063/1.5079292
Submitted: 30 October 2018 · Accepted: 18 January 2019 ·
Published Online: 11 February 2019

D. Shamoon,[1] J. Dermol-Černe,[2] L. Rems,[2] M. Reberšek,[2] T. Kotnik,[2] S. Lasquellec,[1] C. Brosseau,[1,a)] and D. Miklavčič[2]

AFFILIATIONS

[1]Univ Brest, CNRS, Lab-STICC, CS 93837, 6 Avenue Le Gorgeu, 29238 Brest Cedex 3, France
[2]University of Ljubljana, Faculty of Electrical Engineering, Tržaška 25, 1000 Ljubljana, Slovenia

[a)]brosseau@univ-brest.fr

ABSTRACT

In this Letter, we explore how cell electro-deformation and electro-poration are connected. We build a time-domain model of layered concentric shells (a model of biological cells) including their dielectric and elastic properties. We simulate delivery of one trapezoidal voltage pulse to either a single spherical cell or an assembly of three neighboring cells in a specific configuration and calculate cell deformation and pore formation. We describe the qualitative features of the electric field, surface charge density, transmembrane voltage, cell elongation, and pore density distribution at specific times i.e., before, during and after the application of the electric pulse and explore the correlations between them. Our results show that (1) the polarization charge redistribution plays a significant role in the spatial distribution of electrical stresses at μs time scales and (2) the cell deformation and pore density can be correlated with regions of high surface charge density. In future work, our model could be used for understanding basic mechanisms of electro-deformation and electro-poration with high-frequency short bipolar pulses of biological cells in suspension or tissues.

The pursuit of understanding the mechanisms of electro-deformation and electro-poration (EP) of biological cells in suspension or tissue began decades ago[1,2] and the search continues with renewed enthusiasm.[3,4] Understanding the connection between cell electro-deformation and EP is still a relatively unexplored area of research. One of the significant challenges in EP is high molecular weight molecules delivery such as DNA into the living cells. However, most of the existing numerical and analytical studies have tackled the modelling of this phenomenon based on various assumptions and constraints to predict and evaluate cell and tissue EP.[1–14] Typically, EP takes place when the transmembrane potential (TMP) exceeds a threshold V_{ep} above which electrically conductive pores start forming in the membrane.[1–3] Experimental estimates for V_{ep} fall in the range of 0.5–1.2 V but theoretical estimates point to $V_{ep} = 0.258$ V.[15] Most of the existing studies have so far assumed that cell membranes are rigid. This is valid assuming the electro-deformation is much slower in time as compared to the formation of pores. Cells change shape during the application of μs duration pulses and relax to their original shape when the external stimuli stop.[16,17] Yet, these volumetric deformations which are ubiquitous in the context of experimental EP, have not gained much attention in numerical models. Figure 1 shows optical microscopy images of two Chinese Hamster Ovary (CHO) cells from a time-lapse imaging (Multimedia view) of five cells. The applied electric field direction is shown in the middle snapshot. A CHO cell is observed to elongate up to 55% of its initial radius in the direction of the neighboring cell during application of a 100 μs long trapezoidal pulse. After the end of the pulse, the cell returns gradually to its initial shape. Elongation decreases from 55% to 28% in the next 100 μs after the pulse, to 8% after 1 ms and to 5% after 2 ms. It is noteworthy that in physiological experimental conditions, the electro-deformation is much smaller than the present case which may not be captured unless more advanced ultrafast imaging is used.

In this Letter, 3-D finite-element method is used to simulate the time-dependent electro-deformation and EP of a

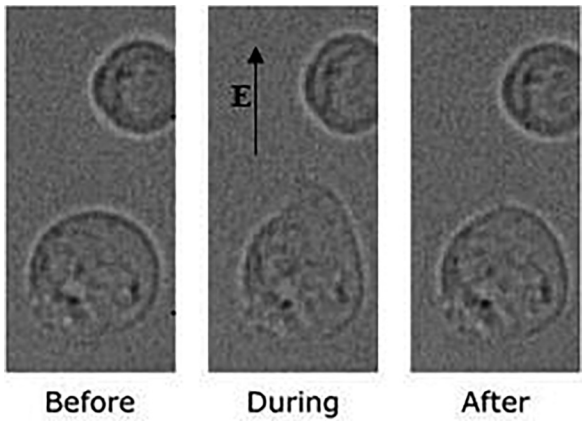

FIG. 1. Snapshots from the time-lapse of CHO cells treated with a 100 μs long pulse (for details on the experimental setup, see supplementary material). Multimedia view: https://doi.org/10.1063/1.5079292.1

single-cell and an assembly of three cells in a specific configuration when one trapezoidal pulse is delivered. Specifically, we borrow from the existing research (see, e.g., Refs. 3, 7, 18, and 19) on the DeBruin and Krassowska asymptotic model of EP for a single cell based on the Smoluchowski equation which is solved on the cell surface to give pore density. The surface patterns of various important quantities like the electric field and surface charge density, Maxwell stress tensor (MST), TMP and pore density are examined at specific times, i.e., at the beginning, during and the end of the pulse. The main innovation of this Letter is to evaluate the correlation between the electric field, TMP, surface charge, and pore density distributions at the cell surface. This modelling is motivated in part by the recently proposed irreversible EP with high-frequency short bipolar pulses[11,12] that reduces the occurrence of muscle contractions during clinical therapy showing that it is of utmost importance to consider the physical forces that govern cell deformation in order to optimize the EP efficiency.[4] We also note that other authors have proposed interesting 3D models of simple or realistically shaped cells in densely packed tissues.[11–14,19,20]

We use a model characterized by a principle of minimality in many respects. As in Refs. 21–23, the electrical properties are deduced from a core-shell modelling. In the case which is considered here, the elastic properties of cells are assumed to be spatially uniform, i.e., both cell and suspension medium have the same properties. Two reasons that spatially uniform properties are used here are that we already know that the mechanical properties of cells remain poorly understood fundamentally[16,17] and the cell cytoplasm contains an elastic cytoskeleton while the cell exterior may contain an elastic matrix in the case of tissue or less of this in case of suspension media, all of which are too complex to be a part of this model. The purpose of our model remains to highlight some specific features in the results irrespective of the complexity of either the mechanical model or poration model used. Several factors can influence the distribution of electrical stress over the membrane such as the membrane compositional heterogeneity or different conductivity ratio across the membrane. In this work, we are focused in a particular scenario but such a model raises the question of how the electrical stress induced deformation of the cell would affect the final relaxation state when the electrical pulse delivery is finished. Furthermore, we expect the EP behavior is similar to that observed in previous studies so we can approximate the membrane conductivity by $\sigma(t) = N(t)\left(2\pi r_p^2 \sigma_p d_m/(\pi r_p + 2d_m)\right)$, where we denote the pore density in the cell membrane, the radius and the internal electrical conductivity of a single pore, and the membrane thickness by N, r_p and σ_p, and d_m, respectively.[18] In Refs. 15 and 18 (see also references therein), it was shown that one can extract information about pores by solving a differential equation that governs the dynamics of the pore density as a function of time t, $\dot{N}(t) = \alpha \exp\left((TMP/V_{ep})^2\right)[1 - (N(t)/N_0)\exp\left(-q(TMP/V_{ep})^2\right)]$, where N_0 is the pore density in the non-electroporated membrane, while α and q are two parameters describing the EP process.

Our starting point is to consider a single spherical cell (at rest) and an assembly of three cells in a specific configuration (Fig. 2) that are exposed to a positive polarity trapezoidal voltage pulse (applied in the z-direction) which delivers an average electric field of strength $E_0 = 5$ kV/cm. Of course, one could also consider the case of a multicellular environment modelling tissue,[9] an interesting generalization that we will discuss later. The electric and elastic properties are given as input parameter values for our simulations (see supplementary material). First, the Laplace equation is solved for electric potential, and then MST is calculated at the cell membrane as $MST_{ij} = \varepsilon\left(E_i E_j - \frac{1}{2}\delta_{ij}E^2\right)$ where i, j can be x, y, and z, E is the electric field, and ε is the membrane permittivity. In this, the surface electric field is obtained from the solution of electric potentials that are coupled at the cell membrane through a boundary condition $\boldsymbol{n}.\boldsymbol{J} = \frac{1}{d_m}\left(\sigma - \varepsilon\frac{\delta}{\delta t}\right)(V_{int} - V_{ext})$ where $\boldsymbol{J}$ is the current density $\boldsymbol{n}$ the outward normal from the cell, d_m is the membrane thickness, σ is the membrane conductivity, and "int" and "ext" denote the cell interior and exterior, respectively. The average electric stretching force experienced by upper or the lower half of the reference cell is within the range of 0.1–0.3 nN. The MST distribution over the cell surface is an input parameter of the elastic model, which solves the time evolution of cell shape. The polarization charge redistribution induces stresses and changes the initially spherical surface of the cell into a prolate shaped surface. For a 6 μm cell radius (R), the electro-deformation $\Delta R/R$, gradually increases the dimension along the z-axis. In our example model, the pulse delivery begins at t = 10 μs and is finished at 110 μs to achieve good electrostatics. The total simulation runtime is 200 μs.

Simulations are performed using COMSOL Multiphysics® v5.2.[24] The simulations use a $50 \times 50 \times 50$ μm^3 computational domain with electrically insulated boundary conditions for the y-z and x-z planes (conservation of the electric current density), adopting previously published techniques.[4,8,9,23] Tetrahedral meshes are used in our calculations. The number of tetrahedral elements varies between 16 570 (single-cell) and 19 320 (3-cell configuration). The membrane is replaced by a thin surface to which a boundary condition is assigned between the cytoplasm

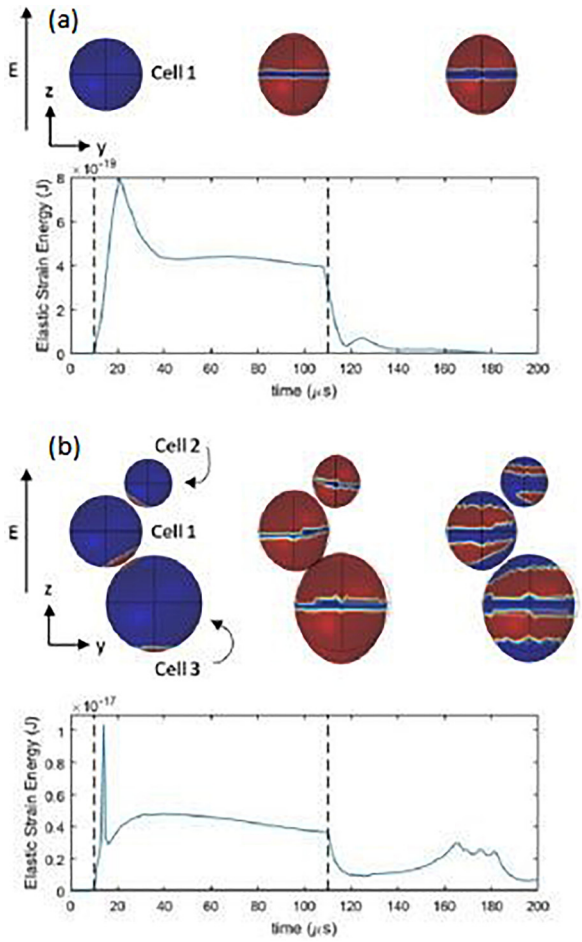

FIG. 2. Simulation results highlighting the trends of the total elastic strain energy in (a) single and (b) 3-cell configurations versus time. The pulse begins at 10 μs and ends at 110 μs—the limits of the pulse are marked with vertical dashed lines. The 3-dimensional plots represent the areas corresponding to TMP $\geq V_{ep} = 0.258$ V (shown in red, otherwise blue) at t = 10 μs (left), t = 109 μs (middle), and t = 112 μs (right). The radii for cells 1–3 are 6, 4, and 8 μm, respectively. Multimedia views: https://doi.org/10.1063/1.5079292.2; https://doi.org/10.1063/1.5079292.3

and the extracellular medium.[4,9] The average computational time of a typical simulation is about 13 min for a single cell and 38 min for three cells on Intel® Core™ i7–5500U CPU.

Figure 2 (Multimedia views) shows the area corresponding to TMP $\geq V_{ep}$ in red color, starting from the poles, then spreading with time to other regions of the cell surface except near the equator ($\theta = \pi/2$), and then shrinking once the pulse is finished. Charge distribution induces asymmetry along the z-direction, and the appearance of the characteristic prolate-shaped cells is observed as those shown experimentally in Fig. 1. These plots are interesting because a possible indirect detection of EP is that a large rise in the surface charge density is seen once the TMP exceeds V_{ep} corresponding to the induced buildup of charges across the cell membrane. We now describe the temporal dynamics of the elastic strain energy which is equivalent to the potential energy stored in the material when it is stretched with a force. Within this elastic model, the strain energy follows the voltage excitation up to a maximum, then shows a relaxation followed by a plateau, and has a complex behavior when the pulse is finished depending on the induced buildup of charges across the cell membrane. This is reasonable because we expect that the charge relaxation process for longer times (>100 μs) is describable by reversible physics. There is another noticeable point, i.e., the strain energy is two orders of magnitude weaker for the single cell configuration compared to the multiple cell one. Since strain energy represents the energy absorbed in the structure when strained, the larger number of cells the larger energy strain.

Besides determining the dependence of the cell elongation perpendicular to the high electric field regions over the membrane, such calculations can also serve to direct access into the symmetries of the surface charge and pore density and to achieve a correlation between them. The TMP is most naturally described in terms of the Maxwell-Wagner-Sillars interfacial polarization of the membrane. The TMP caused by the delivery of external electric field scales with time as $\propto E_0 R \cos(\theta)[1 - \exp(-t/\tau)]$, where $\tau \propto \sigma^{-1}$ is the time constant of membrane charging. For a single cell configuration (Fig. 3, left column), θ is a polar angle

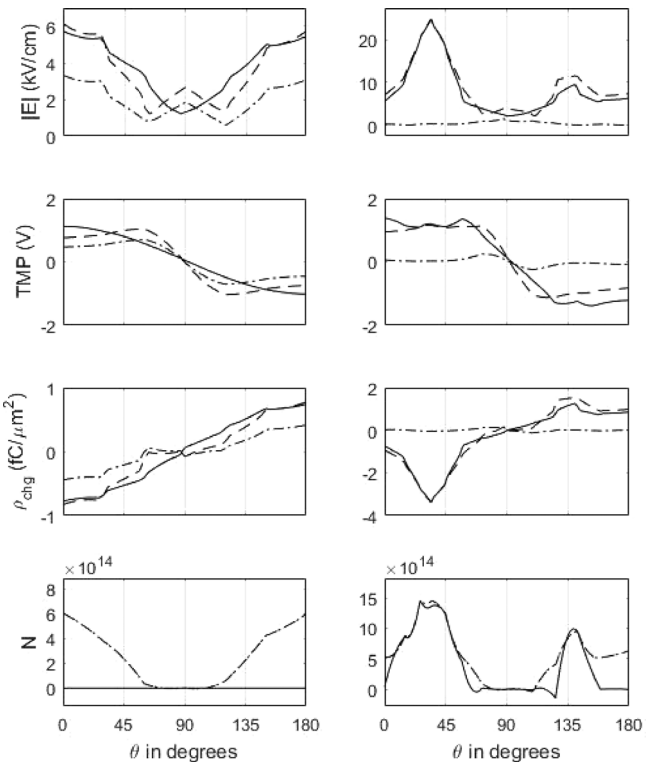

FIG. 3. Comparison of the (y-z) plane distribution of the electric field norm, TMP, surface charge, and pore density of the single (left) and three-cell (right) in suspension at specific times of the electric pulse: t = 11 μs (solid line), t = 109 μs (dashed line), and t = 112 μs (dash-dotted line). θ is a polar angle measured from the center of the cell 1 (of radius 6 μm) going counterclockwise from the –z to the +z direction.

measured from the center of the cell 1 (of radius 6 μm) going counterclockwise from the −z to the +z direction. To further explore how redistribution of polarization charges can be contrasted with the single cell case, we now consider a 3-cell configuration. For the 3-cell configuration (Fig. 3, right column), θ is defined with respect to cell 1 as before. Cell 2 has a radius of 4 μm and cell 3 has a radius of 8 μm. The initial gap distances between the closest points of cell 2 and cell 3 surfaces with respect to cell 1 are 630 nm and 420 nm, respectively. The results in Fig. 3 show the asymmetry of the electric field norm, TMP, surface charge density, and pore density.

We first consider a single spherical cell in suspension (Fig. 3, left column) and make some consistency checks, i.e., at 11 μs, one finds a cosine law dependence of the electric field. A closer look at the pore density shows that once pores are created the highest density remains localized at the polarized poles. In our calculations for the 3-cell configuration, the electric field norm shows two peaks. The results show that the angle for the higher peak corresponds to the larger cell and the other peak corresponds to the smaller cell. It is also useful to look at the surface charge density: in the isolated cell case, it correlates well with TMP, but for the 3-cell configuration it correlates with high electric field areas. From the right column of Fig. 3, we also note that there is a coincidence of the extrema of the electric field, TMP, and pore density. Such behavior has been corroborated experimentally in red blood cells as well as in supramolecular giant unilamellar lipid vesicles.[4] Additionally, the remarkable aspect of this geometry is that it can give rise to the Coulomb repulsion-to-attraction transition when very closely approaching a pair of static bodies having dissimilar surface potentials, a phenomenon associated with an asymmetric electrostatic screening at very small separation between cells.[25] From the perspective of generating a cell hierarchy for tissue modelling, the important aspect of this geometry is that it allows simultaneously analyzing proximity, crowding, and correlation effects between cells.

To further challenge our simulation data, in Fig. 4, we plot the MST distribution and elongation δy and δz in the y- and z-directions, respectively.

Firstly, proximity effects lead to distortions of the spatial distributions of δy and δz. Especially instructive is the clearly established correlation between the MST distribution and elongation in the y and z directions as presented in the right column of Fig. 4. The fact that simulations see a much better alignment of these quantities in the direction of the maximum electric field is reflective of the interplay between the surface charge distribution and the mechanical restoring forces of the cell in our model. When the number of cells in proximity is large, it is expected to have the following behavior: the larger local electric field, the more pronounced pore formation.

In summary, this study reveals some of the subtleties of cell electrostatics and mechanics, either for a spherical cell or an assembly of 3-cells in a specific configuration, that involve a complex interplay of the effects of the electric field, cell surface charge, TMP, pore density, and characteristics of the delivered pulse. Together, these observations suggest that the spatial organization of the polarization charges can play an important

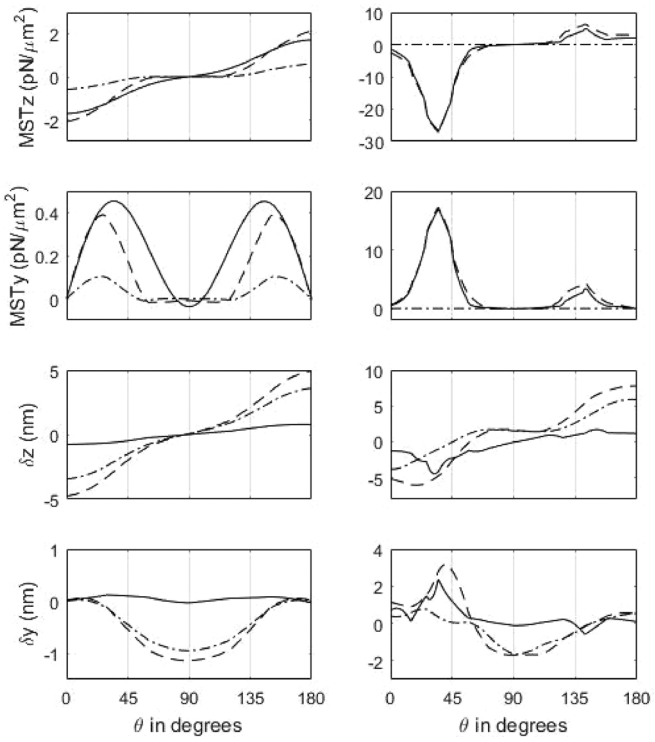

FIG. 4. As in Fig. 3 for the MST distribution and elongation in the y- and z-directions, respectively.

role in electro-deformation and EP of biological cells and that this organization can be controlled to facilitate EP. Our model can also be extended in directions such as linking to various device configurations with microfluidics and transport of dilute species from the cell exterior to its interior or vice-versa. This will render the extended models more appropriate for experimental validations with existing studies.[26] A two-dimensional model describing several irregularly shaped cells in proximity has recently been studied by Mescia and co-workers.[27]

From a physical perspective, it is important to note that some EP models incorporate the change in the membrane tension due to the presence of pores which might also affect membrane elasticity. A more refined elastic model of the cell treating the contributions of the actomyosin cytoskeleton to the cell size and shape variations under external electric perturbation is required for a broader perspective. In particular, we plan to include the effect of cytoskeletal structures since the tensegrity architecture is a fundamental principle that governs how real cells are structured to respond biomechanically to mechanical forces. It is also worth mentioning that electric pulses leading to EP have an effect on the integrity of the cytoskeleton.[28] From a biophysics perspective, our study sets the stage to explore more complicated coarse-grained models that generate dense heterogeneous and anisotropic tissues such as in Ref. 8. Also, different kinds of voltage excitation, e.g., high-frequency short bipolar pulses need special attention. Such features will be considered in future work.

See supplementary material contains the details of the experimental setup and the list of parameters used in our model.

This work was partially supported by the Université de Brest through its mobility program. The Lab-STICC is the Unité Mixte de Recherche CNRS 6285. This work is also partially supported by the Slovenian Research Agency (research core Funding Nos. P2-0249 and IP-0510). The research is conducted within the scope of the electroporation in the Biology and Medicine (EBAM) European Associated Laboratory (LEA). The Vision Research Phantom v2010 camera was kindly provided by Vision Research Europe.

REFERENCES

[1]D. S. Dimitrov, "Electroporation and electrofusion of membranes," in *Handbook of Biological Physics*, edited by R. Lipowsky and E. Sackmann (Elsevier, Amsterdam, 1995), Vol. 1B, pp. 851–901.
[2]J. C. Weaver and Y. A. Chizmadzhev, "Theory of electroporation: A review," Bioelectrochem. Bioenergy **41**, 135–160 (1996).
[3]L. Rems and D. Miklavčič, "Electroporation of cells in complex materials and tissue," J. Appl. Phys. **119**, 201101 (2016).
[4]E. Goldberg, C. Suárez, M. Alfonso, J. Marchese, A. Soba, and G. Marshall, "Cell membrane electroporation modeling: A multiphysics approach," Bioelectrochemistry **124**, 28–39 (2018).
[5]M. Bier, W. Chen, T. R. Gowrishankar, R. D. Astumian, and R. C. Lee, "Resealing dynamics of a cell membrane after electroporation," Phys. Rev. E **66**, 062905 (2002).
[6]C. Chen, S. W. Smye, and M. P. Robinson, "Membrane electroporation theories: A review," Med. Biol. Eng. Comput. **44**, 5–14 (2006).
[7]G. Pucihar, D. Miklavčič, and T. Kotnik, "A time-dependent numerical model of transmembrane voltage inducement and electroporation of irregularly shaped cells," IEEE Trans. Biomed. Eng. **56**, 1491–1501 (2009).
[8]T. Murovec, D. C. Sweeney, E. Latouche, R. V. Davalos, and C. Brosseau, "Modeling of transmembrane potential in realistic multicellular structures before electroporation," Biophys. J. **111**, 2286–2295 (2016).
[9]M. Essone Mezeme, G. Pucihar, M. Pavlin, C. Brosseau, and D. Miklavčič, "A numerical analysis of multicellular environment for modeling tissue electroporation," Appl. Phys. Lett. **100**, 143701 (2012); See also M. Essone Mezeme, M. Kranjc, F. Bajd, I. Sersa, C. Brosseau, and D. Miklavčič, "Assessing how electroporation affects the effective conductivity tensor of biological tissues," Appl. Phys. Lett. **101**, 213702 (2012).
[10]H. Isambert, "Understanding the electroporation of cells and artificial bilayer membranes," Phys. Rev. Lett. **80**, 3404 (1998).
[11]H. Li, A. Denzi, X. Ma, X. Du, Y. Ning, X. Cheng, F. Apollonio, M. Liberti, and J. C. M. Hwang, "Distributed effect in high-frequency electroporation of biological cells," IEEE Trans. Microwave Theory Tech. **65**, 3503–3511 (2017); S. Dong, H. Wang, Y. Zhao, Y. Sun, and C. Yao, "First human trial of high-frequency irreversible electroporation therapy for prostate cancer," Technol. Cancer Res. Treat. **17**, 1–9 (2018); B. Valič, M. Golzio, M. Pavlin, A. Schatz, C. Faurie, B. Gabriel, J. Teissié, M. Rols, and D. Miklavčič, "Effect of electric field induced transmembrane potential on spheroidal cells: Theory and experiment," Eur. Biophys. J. **6**, 519–528 (2003).
[12]C. B. Arena, M. B. Sano, M. N. Rylander, and R. V. Davalos, "High-frequency irreversible electroporation (H-FIRE) for non-thermal ablation without muscle contraction," IEEE Trans. Biomed. Eng. **58**, 1474–1481 (2011); D. C. Sweeney, M. Reberšek, J. Dermol, L. Rems, D. Miklavčič, and R. V. Davalos, "Quantification of cell membrane permeability induced by monopolar and high-frequency bipolar bursts of electrical pulses," Biochim. Biophys. Acta (BBA)-Biomembr. **11**, 2689–2698 (2016); L. Mescia, M. A. Chiapperino, P. Bia, J. Gielis, and D. Caratelli, "Modeling of electroporation induced by pulsed electric fields in irregularly shaped cells," IEEE Trans. Biomed. Eng. **65**, 414–423 (2018).
[13]E. C. Gianulis, M. Casciola, S. Xiao, O. N. Pakhomova, and A. G. Pakhomov, "Electropermeabilization by uni- or bipolar nanosecond electric pulses: The impact of extracellular conductivity," Bioelectrochemistry **119**, 10–19 (2018).
[14]V. Novickij, P. Ruzgys, A. Grainys, and S. Šatkauskas, "High frequency electroporation efficiency is under control of membrane capacitive charging and voltage potential relaxation," Bioelectrochemistry **119**, 92–97 (2018); J. Dermol and D. Miklavčič, "From cell to tissue properties—modeling skin electroporation with pore and local transport region formation," IEEE Trans. Biomed. Eng. **65**, 458–468 (2018).
[15]K. A. DeBruin and W. Krassowska, "Modeling electroporation in a single cell. I. Effects of field strength and rest potential," Biophys. J. **77**, 1213–1224 (1999); , "Modeling electroporation in a single cell. II. Effects of ionic concentrations," **77**, 1225–1233 (1999); J. C. Neu and W. Krassowska, "Asymptotic model of electroporation," Phys. Rev. E **59**, 3471–3482 (1999).
[16]B. Varga, C. Fazakas, I. Wilhelm, I. A. Krizbai, Z. Szegletes, G. Váró, and A. G. Végh, "Elasto-mechanical properties of living cells," Biochem. Biophys. Rep. **7**, 303–308 (2016).
[17]M.-A. Meyers, P.-Y. Chen, A. Y.-M. Lin, and Y. Seki, "Biological materials: Structure and mechanical properties," Prog. Mater. Sci. **53**, 1–206 (2008).
[18]L. Rems, "Cell electrofusion using nanosecond electric pulses," Sci. Rep. **3**, 3382 (2013); J. Li and H. Lin, "Numerical simulation of molecular uptake via electroporation," Bioelectrochemistry **82**, 10–21 (2011).
[19]D. Voyer, A. Silve, L. M. Mir, R. Scorretti, and C. Poignard, "Dynamical modeling of tissue electroporation," Bioelectrochemistry **119**, 98–110 (2018); G. Pucihar, T. Kotnik, B. Valič, and D. Miklavčič, "Numerical determination of transmembrane voltage induced on irregularly shaped cells," Ann. Biomed. Eng. **34**, 642 (2006).
[20]D. Shamoon, S. Lasquellec, and C. Brosseau, "Perspective: Towards understanding the multiscale description of cells and tissue by electromechanobiology," J. Appl. Phys. **123**, 240902 (2018).
[21]R. Pethig, *Dielectric and Electronic Properties of Biological Materials* (Wiley, New York, 1979).
[22]M. R. Willis, "Dielectric and Electronic Properties of Biological Materials' by R Pethig. pp 376. John Wiley & Sons, Chichester and New York. 1979. £15," [book review], Biochem. Educ. **8**(1), 31 (1980).
[23]M. Essone Mezeme and C. Brosseau, "Simulation of a toy model of cylindrical cells submitted to nonionizing electromagnetic field: Effect of membrane cell disruption," J. Appl. Phys. **107**, 014701 (2010).
[24]COMSOL Multiphysics version 5.2.
[25]T. Murovec and C. Brosseau, "Anisotropy of the crossover between electrostatic attraction and repulsion of biological cells," Appl. Phys. Lett. **103**, 193702 (2013).
[26]Y. Zhan, C. Sun, Z. Cao, N. Bao, J. Xing, and C. Lu, "Release of intracellular proteins by electroporation with preserved cell viability," Anal. Chem. **84**, 8102 (2012); B. del Rosal, C. Sun, D. N. Loufakis, C. Lu, and D. Jaque, "Thermal loading in flow-through electroporation microfluidic devices," Lab Chip **13**, 3119 (2013); T. Geng and C. Lu, "Microfluidic electroporation for cellular analysis and delivery," Lab Chip **13**, 3803 (2013).
[27]L. Mescia, M. A. Chiapperino, P. Bia, C. M. Lamacchia, J. Gielis, and D. Caratelli, "Design of electroporation process in irregularly shaped multicellular systems," Electronics **8**, 37 (2019).
[28]T. Kotnik, L. Rems L, M. Tarek, and D. Miklavčič, "Membrane electroporation and electropermeabilization: Mechanisms and models," Annu. Rev. Biophys. (in press).